

# Improved Sensitivity in Selective NMR Correlation Spectroscopy and Applications to the Determination of Scalar Couplings in Peptides and Proteins

Pierre Borgnat,<sup>‡</sup> Anne Lesage,<sup>‡</sup> Stefano Caldarelli,<sup>†</sup> and Lyndon Emsley<sup>\*,‡</sup>

Contribution from the Laboratoire de Stéréochimie et des Interactions Moléculaires, UMR-117 CNRS/ENS, Ecole Normale Supérieure de Lyon, 69364 Lyon, France, and Section de Chimie, Université de Lausanne, CH-1015 Lausanne, Switzerland

Received April 8, 1996<sup>⊗</sup>

**Abstract:** A new method, providing a significant improvement in sensitivity, is presented for obtaining selective two-dimensional NMR correlation (COSY) spectra. The method is demonstrated on a small molecule having nonlinear optical properties and is further demonstrated by the precise determination of scalar coupling constants in the peptide gramicidin and in a 57 amino acid fragment of the nucleocapsid of the hepatitis C virus. In these systems we observe sensitivity improvements of between a factor of 2 and 6. In the case of the protein it was not practical to record the selective COSY spectra using conventional techniques. The method makes use of the recently introduced concept of “linear” selective pulses which provide a simple way of obtaining pure-phase band selective excitation with an arbitrary shape for the response. In a selective 2D COSY experiment the relative sensitivity improvement provided by these pulses is cubed with respect to a 1D experiment. The resulting pulse sequences are highly unusual in that they require a modulation of the pulse shape and pulse length as the indirect detection period is increased.

## Introduction

Selective two-dimensional NMR correlation spectroscopy (COSY) and related experiments have been demonstrated to provide particularly simple methods of accurately measuring homonuclear scalar coupling constants and thus of determining structural features in relatively small molecules.<sup>1,2</sup> However, the application of such techniques to large molecular systems, such as proteins or nucleic acid fragments containing more than about 10 base pairs, is limited to a small handful of isolated examples.<sup>3,4</sup> This is primarily due to problems associated with the relatively short transverse relaxation times in such molecules.

By their very nature selective pulses are relatively long. Selective excitation is achieved by applying a long low-power pulse in place of the ordinary short high-power pulse,<sup>5–8</sup> and the bandwidth of excitation is inversely proportional to the pulse length (an expression of the uncertainty relation for NMR). Thus, a pulse length of about 60 ms is required to excite a spectral region of about 50 Hz. The form of the frequency-domain response varies according to the shape of the pulse used, and the exact length of the pulse depends on the shape. The value of 60 ms corresponds to an excitation bandwidth of 50 Hz for

a sinc shaped pulse truncated after three zero crossings on each side of the maximum. Such pulse lengths become comparable to the transverse relaxation times in large molecules, leading to seemingly unavoidable reduction in the signal-to-noise ratio of the spectrum due to the decay of magnetization during the pulse. For example, a transverse relaxation time of about 60 ms corresponds to a line width of 5 Hz (which is by no means unusual).

In this article we introduce a new approach to selective correlation spectroscopy which largely overcomes these disadvantages and can lead to more than a 5-fold improvement in signal-to-noise ratios in macromolecular samples, which in turn corresponds to a 25-fold reduction in the experimental time required to obtain a given signal-to-noise ratio. This improvement has allowed us to record, by way of example, NH- $\alpha$  cross peaks in a peptide and a protein. These measurements were not practicable using the conventional approach to selective COSY. The cross peaks allow us to measure precisely (in this case  $\leq \pm 0.3$  Hz) the three-bond scalar couplings which define the conformation of the protein backbone.

## Linear Selective Pulses

We have recently introduced the idea of using simple pulse shapes for selective excitation in NMR whose frequency domain response can be predicted by Fourier transformation of the time-domain envelope.<sup>9</sup> This leads to the suggestion that Gaussian or sinc shaped pulses (amongst others) should be useful excitation functions since, for example, the Fourier transformation of a sinc function is a “top-hat.” However, such excitation functions normally lead to a large phase dispersion in the response. The use of such functions as sinc or Gaussian to obtain a pure-phase response is made possible through the action of starting the acquisition of the signal *in the middle of the pulse*. This is suggested by consideration of Fourier transform theory which shows that the origin of the phase dispersion observed after a small flip angle pulse is at the origin of the excitation function, which for a symmetric pulse is given by  $\tau_{\text{focus}} = 1/2\tau_p$ .

\* To whom correspondence should be addressed.

<sup>†</sup> Université de Lausanne.

<sup>‡</sup> Laboratoire de Stéréochimie et des Interactions Moléculaires.

<sup>⊗</sup> Abstract published in *Advance ACS Abstracts*, September 1, 1996.

(1) Kessler, H.; Anders, U.; Gemmecker, G.; Steuernagel, S. *J. Magn. Reson.* **1989**, *85*, 1.

(2) Emsley, L. Shaped Selective Pulses and their Applications in Assignment and Structure Determination by NMR. In *Nuclear Magnetic Resonance, Part C, A Volume of Methods in Enzymology*; James, T. L., Oppenheimer, N. J., Ed.; Academic Press: Orlando, 1994.

(3) Emsley, L.; Dwyer, T. J.; Spielmann, H. P.; Wemmer, D. E. *J. Am. Chem. Soc.* **1993**, *115*, 7765.

(4) Boulat, B.; Burghardt, I.; Bodenhausen, G. *J. Am. Chem. Soc.* **1992**, *114*, 10679.

(5) Warren, W. S.; Silver, M. S. *Adv. Magn. Reson.* **1988**, *10*, 1.

(6) Freeman, R. *Chem. Rev.* **1991**, *91*, 1397.

(7) Emsley, L. Selective Pulses In *The Encyclopedia of NMR*; Grant, D. M., Harris, R. K., Ed.; J. Wiley & Sons: London, 1995.

(8) Warren, W. S. Shaped Pulses In *The Encyclopedia of NMR*; Grant, D. M., Harris, R. K., Ed.; J. Wiley & Sons: London, 1995.

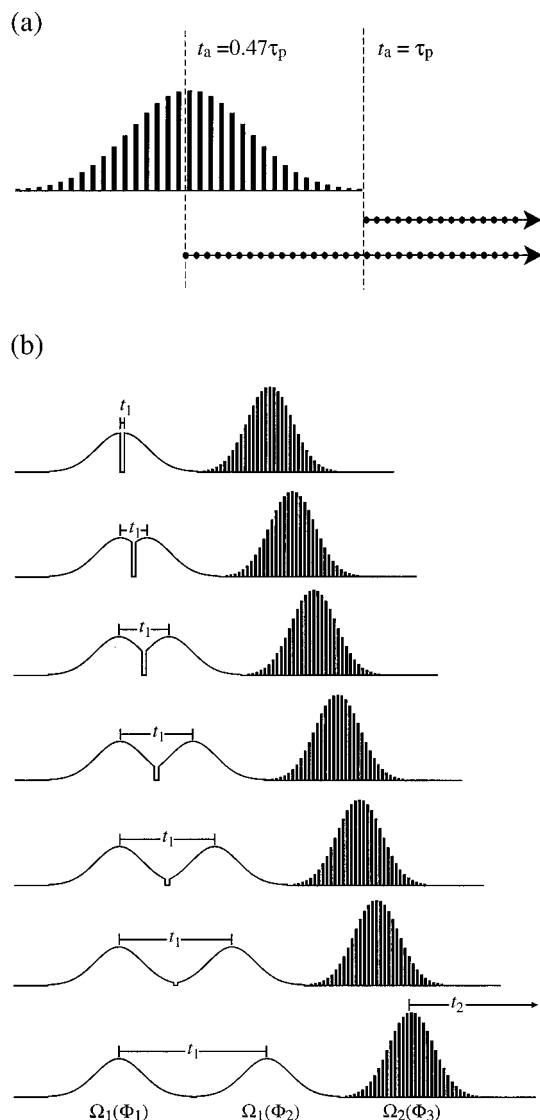


**Figure 1.** Pulse sequences involving the PARADISE acquisition scheme. (a) One-dimensional PARADISE acquisition scheme. The pulse is implemented using the DANTE technique,<sup>10,11</sup> and in this case the amplitude is modulated according to a Gaussian function. Acquisition is normally started at the end of the pulse, but if acquisition is started halfway through the pulse, with the acquisition being synchronized with the “windows” in the pulse, a pure-phase response is achieved.<sup>9</sup> (b) The pulse sequence suitable for two-dimensional selective COSY using retroactive acquisition in both dimensions. See text for details.

This observation leads to the concept of a virtual focus (first introduced by R. Freeman) of the magnetization at the center of the pulse. In a recent communication<sup>9</sup> we demonstrated that this idea can be realized in simple one-dimensional experiments by using a DANTE implementation<sup>10,11</sup> of the pulse shape in which the “windows” in the pulse allow the acquisition of the points which fall during the pulse, as illustrated in Figure 1. This turns out to provide an extremely versatile method of selective excitation in which the frequency-domain response can be arbitrarily tailored simply by using excitation functions which are the inverse Fourier transform of the desired response. In this way we have recently introduced a series of new excitation pulses adapted from ordinary filter functions, including such shapes as cosine, Hanning, hamming, and sinc, whose various

(9) Caldarelli, S.; Lesage, A.; Emsley, L. *J. Magn. Reson. A* **1995**, *116*, 129.

(10) Bodenhausen, G.; Freeman, R.; Morris, G. A. *J. Magn. Reson.* **1976**, *23*, 171.

(11) Morris, G. A.; Freeman, R. *J. Magn. Reson.* **1979**, *29*, 433.

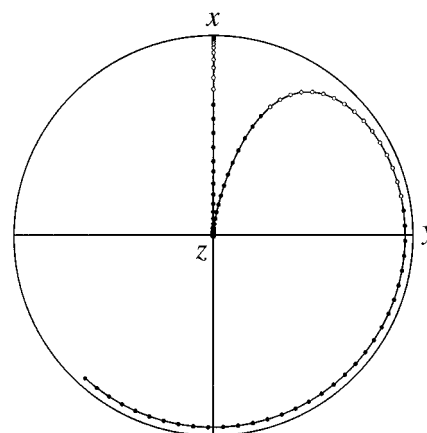


**Figure 2.** Magnetization trajectories projected onto the  $xy$  plane during a Gaussian shaped pulse. As expected the on-resonance magnetization is transformed from the  $z$  axis to the  $x$  axis, where it stays during the acquisition period. The off-resonance trajectory can be divided into three steps. First, (filled circles) there is the evolution during the first half of the pulse; second, (open circles) there is the evolution during the second half of the pulse, corresponding to points that would be acquired in a PARADISE experiment; and, third, there are the points that fall during the following free precession period (filled circles) which correspond to the normal free-induction decay. See text for an interpretation of these trajectories.

excitation properties fulfill differing requirements for the time-domain response.<sup>12</sup> Notably, the cosine-bell shaped pulse was shown to provide a particularly narrowband response for a given pulse length. Because these pulses are suggested by a linear approximation for the NMR response we refer to them as “linear” selective pulses. The one-dimensional method of acquisition is referred to as PARADISE (*pure-phase achieved by retroactive acquisition in DANTE implemented selective excitation*).

We remark that all the predictions upon which the PARADISE method is based come from Fourier transform theory which assumes that the NMR response is linear. However, the NMR response is not linear. It may be a little surprising that the method actually works, bearing in mind that in reality the magnetization is not in focus at  $\tau_{\text{focus}}$  or at any other time during the pulse. Indeed it turns out to be difficult to treat the response using an exact theory (except, obviously, by numerical simulations). In fact this is, to our knowledge, the only example in spectroscopy of the application of a nonperiodic time-dependent Hamiltonian during the acquisition of a signal which leads to a useful result. Even if we cannot provide an exact theory, we can at least rationalize the behavior, and Figure 2 provides a visual basis for why the technique works by showing the trajectories of magnetization projected onto the  $xy$  plane of the rotating frame during the pulse. In order to confirm our ideas we should find that the phase and amplitude behavior is as if there was an origin of the free precession signal at the center of the pulse. We immediately see that *to a first approximation* there is little phase evolution during the first part of the pulse and that there is little amplitude modulation during the second part of the pulse.

### Sensitivity Improvements Using Linear Selective Pulses

The principal factor that has limited the application of selective techniques to relatively small molecules is that of sensitivity. As molecular weight increases the line width increases accordingly, and the length of the selective pulses

(12) Borgnat, P.; Lesage, A.; Caldarelli, S.; Emsley, L. *J. Magn. Reson. A* **1996**, *119*, 289.

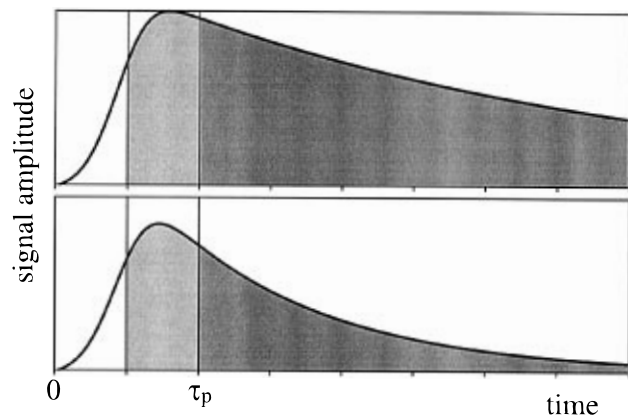


**Figure 3.** Signal intensity of on-resonance magnetization during a Gaussian shaped selective pulse and the following free induction decay for two values of the transverse relaxation time. The signal-to-noise ratio is related to the integral of the signal (and the weighting function).<sup>36</sup> In the upper graph, corresponding to a long  $T_2$ , the contribution of the signal acquired during the pulse (lighter shaded region) is relatively minor compared to the rest of the signal (darker shaded region). In the lower graph, corresponding to a shorter  $T_2$ , however, the contribution of the signal acquired during the pulse represents a much more significant contribution to the overall signal, and it continues becoming increasingly important as  $T_2$  becomes shorter compared to  $\tau_p$ .

becomes nonnegligible when compared to the transverse relaxation time. Under such conditions selective pulse experiments become impractical using conventional techniques because of the loss of signal due to the decay of magnetization during the pulse. A secondary factor that reduces sensitivity is that the line width becomes comparable to the coupling constant in very large molecular systems, leading to cancellation of the signal in COSY type experiments. This factor is equally important in nonselective experiments, and the contribution of the loss due to long pulse lengths can be appreciated if we consider that for many medium sized proteins COSY cross peaks are observed in nonselective experiments, but they are not observed (within practical acquisition times) in soft-COSY experiments.

Having determined that the retroactive acquisition does indeed work well, we realize that it has an advantage over conventional acquisition schemes that was not predicted by Fourier arguments in that *the points that are acquired during the pulse contribute significantly to the overall sensitivity of the experiment*. Moreover, it would seem that, as is illustrated schematically in Figure 3, the shorter the transverse relaxation time, and thus the more rapid the decay of the time-domain signal, the greater is the contribution to the sensitivity from points acquired during the pulse.

Figure 4 represents an experimental confirmation of the sensitivity improvement on the excitation profile of a pulse. The figure shows the spectrum of  $\approx 1\%$   $\text{H}_2\text{O}$  in  $\text{D}_2\text{O}$  doped with  $\text{CuSO}_4$  to give a proton line width for the water resonance of about 3.5 Hz corresponding to a  $T_2$  of around 90 ms. The spectra were recorded as a function of the transmitter frequency and represent the "excitation profile" of the pulse. The figure compares the responses obtained for a 70 ms UBURP pulse<sup>13</sup> (which is representative of a range of existing "conventional" pulses<sup>14–22</sup>) and a 70 ms sinc shaped pulse using the PARADISE

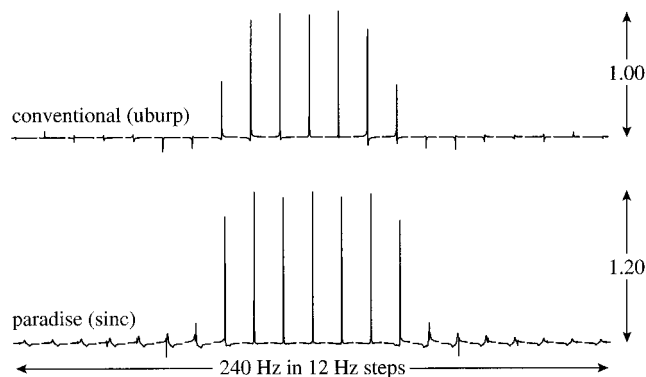


**Figure 4.** Excitation profiles for a sample of 1%  $\text{H}_2\text{O}$  in  $\text{D}_2\text{O}$  doped with  $\text{CuSO}_4$  to give a proton line width of about 3.5 Hz. The excitation profiles are obtained by stepping the carrier frequency (in this case in 12 Hz steps) and recording the spectrum for each different value of the transmitter offset. The figure compares a 70 ms UBURP pulse and a 70 ms sinc shaped pulse using the PARADISE technique. In this case we observe a  $\approx 20\%$  increase in sensitivity for the PARADISE experiment due to the acquisition of the points during the pulse.

technique. In this case the ratio  $\tau_p/T_2 = 0.8$ , and we observe a  $\approx 20\%$  improvement in sensitivity. The sensitivity improvement depends on the ratio  $\tau_p/T_2$ , the larger this ratio the better the *relative* performance of the linear selective pulse.

Note that we have chosen UBURP as a representative "conventional" pure-phase pulse, it is not worse than others in the same genre (such as Gaussian pulse cascades<sup>18</sup>) and performs markedly better than some (notably it has a much smaller bandwidth-duration product than a  $Q^5$  pulse,<sup>19</sup> for example). We chose the UBURP pulse since it has a selectivity comparable to a sinc with three zero crossing on either side of the maximum, and since both pulses provide an almost "top-hat" excitation profile. Also it is one of the rare examples of a "general rotation" pulse,<sup>13,19</sup> making it suitable for use in a soft-COSY experiment.

One might be tempted to think that 20% is a relatively modest increase in sensitivity. However, we shall see in the following sections that this improvement is increased to the third power in a soft-COSY experiment, and that this leads to experimental examples in which the improvement in signal-to-noise ratio is dramatic and is in fact essential to the success of the experiment.

### Pure-Phase Correlation Spectroscopy Using Linear Selective Pulses

A conventional soft-COSY experiment<sup>2,23,24</sup> consists of a first selective pulse applied at the resonance frequency of a first spin and then an *indirect* acquisition period  $t_1$  followed by a second selective pulse applied at the same frequency. The second pulse is in turn immediately followed by a third selective pulse applied at the resonance frequency of a second spin. The third pulse is followed by the *direct* acquisition period  $t_2$ . At first glance it may seem that the implementation of linear selective pulses in a two-dimensional soft-COSY experiment would be hindered, because it appears as if the first two pulses would have to be superimposed upon each other. However, this is not the case as this supposition forgets the discrete, point by point, nature of acquisition used in time-domain NMR experiments.

(18) Emsley, L.; Bodenhausen, G. *Chem. Phys. Lett.* **1990**, *165*, 469.

(19) Emsley, L.; Bodenhausen, G. *J. Magn. Reson.* **1992**, *97*, 135.

(20) Rourke, D. E.; Morris, P. G. *Phys. Rev. A* **1992**, *46*, 3631.

(21) Rourke, D. E.; Morris, P. G. *J. Magn. Reson.* **1992**, *99*, 118.

(22) Shen, J.; Lerner, L. E. *J. Magn. Reson. A* **1995**, *112*, 265.

(23) Brüschweiler, R.; Madsen, J. C.; Griesinger, C.; Sørensen, O. W.; Ernst, R. R. *J. Magn. Reson.* **1987**, *73*, 380.

(24) Cavanagh, J.; Waltho, J. P.; Keeler, J. *J. Magn. Reson.* **1987**, *74*, 386.

(13) Geen, H.; Freeman, R. *J. Magn. Reson.* **1991**, *93*, 93.

(14) Warren, W. S. *Science* **1988**, *242*, 878.

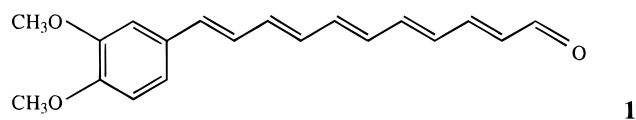
(15) Emsley, L.; Bodenhausen, G. *J. Magn. Reson.* **1989**, *82*, 211.

(16) Morris, P. G.; McIntyre, D. J. O.; Rourke, D. E.; Ngo, J. T. *NMR Biomed.* **1989**, *2*, 257.

(17) Geen, H.; Wimperis, S.; Freeman, R. *J. Magn. Reson.* **1989**, *85*, 620.

The pulse sequence appropriate for soft-COSY using linear selective pulses is given in Figure 1b. The sequence is entirely analogous to a conventional soft-COSY sequence, and the only difference is that the final pulse has been replaced with a PARADISE acquisition and that the first two pulses at the beginning and end of the indirect acquisition period are modulated in shape and duration as a function of  $t_1$ . In a conventional experiment, for example using UBURP pulses or  $270^\circ$  Gaussian pulses, the whole pulse is always applied since the time origin of  $t_1$  is taken to be at the end of the pulse. If we use linear selective pulses the time origin of  $t_1$  is at the center of each pulse. Thus, the first value of  $t_1$  is acquired by applying only the first half of the first pulse, followed by the second half of the second pulse. There is no delay between these two pulses. The second  $t_1$  increment now corresponds to the application of the first half of the first pulse plus an additional fraction of the first pulse corresponding to  $1/2\Delta t_1$ , where  $\Delta t_1$  is the increment of  $t_1$  from one acquisition to the next defining the spectral width in  $\omega_1$ . Similarly the second part of the second pulse is slightly longer, adding a fraction  $1/2\Delta t_1$  so that the total time increment amounts to  $\Delta t_1$ . Once again there is no delay between the two pulses. This manner of incrementing  $t_1$  by increasing the fraction of the pulses that is applied is continued, as illustrated in Figure 1b, until the whole of both pulses are applied, i.e.,  $t_1 = \tau_p$ , and subsequently the experiment is carried out in the "conventional" manner by progressively incrementing the delay between the first and second pulses until the desired  $t_1^{\max}$  (which defines the resolution obtained in  $\omega_1$ ) is obtained. In summary, this manner of incrementing the fraction of the pulse that is applied is exactly analogous, for the indirect detection period  $t_1$ , to the PARADISE technique that is used in  $t_2$ . The pulse in  $t_1$  is not truncated as it might at first sight appear, but the whole pulse is applied (as in  $t_2$ ). The main difference between the two time domains is that both the pulses, on either side of  $t_1$ , must be incremented (since dephasing occurs during both of the pulses). That we should apply the first part of the first pulse and the second part of the second pulse can be appreciated rigorously from symmetry considerations<sup>25</sup> and intuitively by considering that the second pulse transforms transverse magnetization into longitudinal magnetization and therefore that the phase of the transverse magnetization evolves mostly during the first part of the pulse (in analogy to Figure 2, which treats the situation for the transformation of longitudinal magnetization into transverse magnetization, and where the phase evolution is mostly during the second part of the pulse).

Figure 5 shows the experimental realization of this technique to measure the H1-H2 soft-COSY cross peak in the polyene **1**, where the numbering of the protons commences at the right hand side of the chain.



This compound has nonlinear optical properties that depend sensitively on the configuration of the conjugated chain. Measurement of the  $^3J_{\text{HH}}$  scalar couplings is the simplest way to ensure that, in this case, the chain is all *trans*. The upper spectrum in Figure 5 was acquired using the sequence of Figure 1b and sinc shaped pulses and is directly comparable to the lower spectrum which was recorded using  $90^\circ$  sinc-shaped pulses in a conventional soft-COSY experiment. One immediately observes that the phase properties in both dimensions

are excellent with the new method, while, as expected, the conventional technique using sinc-shaped pulses leads to a large phase dispersion in both dimensions. Note that the phase dispersion is expected to be twice as large in  $t_1$  as in  $t_2$  since the phase gradient accumulates during both pulses, at the beginning and end of  $t_1$ , while it accumulates only during the one pulse before  $t_2$ .

Besides the phase properties we notice immediately that there is a nearly twofold increase in sensitivity between the two experiments which is at first sight surprising considering that this is a relatively small molecule with a long  $T_2$  ( $\approx 100$  ms). However, a straightforward consideration of the mechanism of the pulse sequence shows us that any sensitivity increase observed in the one-dimensional experiment is likely to be *cubed* in the two-dimensional experiment. This is because the experiment selects a projection of the magnetization after each pulse. After the first pulse the projection onto the  $xy$  plane is taken (corresponding to the selection of  $p = \pm 1$  quantum coherence),<sup>26</sup> after the second pulse the projection onto the  $z$  axis is chosen (corresponding to the selection of  $p = 0$ ), and only the transverse single quantum coherence is selected during  $t_2$ . This series of projections is therefore multiplicative, and, for example, the factor 1.2 increase in sensitivity observed in the one-dimensional experiment of Figure 4 becomes a  $1.2^3 = 1.7$  increase in sensitivity for the two-dimensional experiment. Indeed the polyene has a  $\tau_p/T_2$  ratio similar to that for the example of Figure 4, and this agrees satisfyingly well with the experimentally observed increase in sensitivity seen in Figure 5. Note that the fact that anti-phase coherences are observed in this experiment does not affect significantly our argumentation since they grow and decay continuously in the same manner as in-phase coherences. The fact that they are affected similarly can be appreciated from the agreement with the predicted behavior.

### Selective Correlation Spectroscopy of Peptides and Proteins

As discussed above, the relative sensitivity improvement obtained by using the sequence of Figure 1 is likely to be greatest in systems with short transverse relaxation times. Thus we have tested the application of the sequences on the peptide gramicidin (15 amino acids) and the protein Capsid(1-48)\* which is the N-terminal region of the nucleocapsid of the hepatitis C virus. The results are shown in Figures 6 and 7. For the 2 mM gramicidin sample a spectacular improvement in signal-to-noise ratio, of between a factor 2 and 5 (depending on the particular spectrum), is observed. Gramicidin represents a molecular weight at the upper limit of the applicability of soft-COSY using conventional acquisition schemes. As can be appreciated from the comparison spectra shown in Figure 6, the technique of Figure 1 yields an order of magnitude reduction of the experimental time required to obtain a spectrum with good signal to noise. The spectra shown are of sufficient quality to yield very precise values of the  $^3J_{\text{NH-H}\alpha}$  coupling constants (which, through the Karplus relation,<sup>27-31</sup> yield the backbone torsion angles  $\phi$ ) and the  $^3J_{\text{H}\beta\text{-H}\alpha}$  coupling constants which are also manifested in these spectra. The values of the coupling constants were obtained by iterative fitting of the soft-COSY

(26) Bodenhausen, G.; Kogler, H.; Ernst, R. R. *J. Magn. Reson.* **1984**, *58*, 370.

(27) Karplus, M. *J. Chem. Phys.* **1959**, *30*, 11.

(28) Karplus, M. *J. Am. Chem. Soc.* **1963**, *85*, 2870.

(29) Wüthrich, K. *NMR of Proteins and Nucleic Acids*; Wiley: New York, 1986.

(30) *NMR of Macromolecules. A Practical Approach*; Roberts, G. C. K., Ed.; Oxford University Press: Oxford, 1993.

(31) Eberstadt, M.; Gemmecker, G.; Mierke, D. F.; Kessler, H. *Angew. Chim. Int. Ed. Engl.* **1995**, *34*, 1671.

(25) Ngo, J. T.; Morris, P. G. *J. Magn. Reson.* **1987**, *75*, 122.

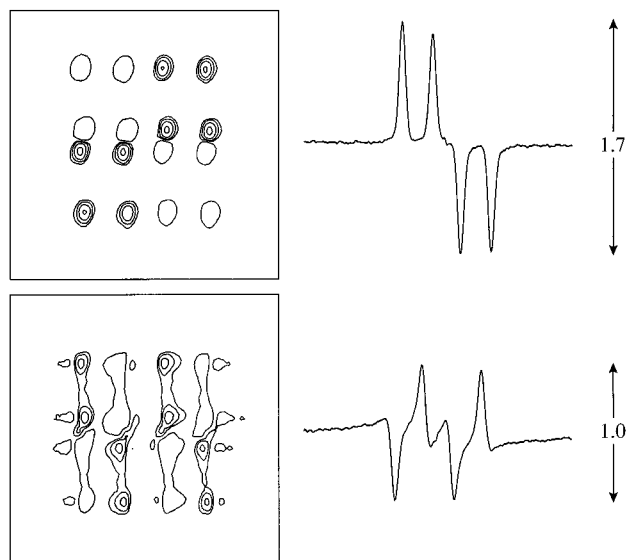


**Figure 5.** Selective COSY spectra for a sample of **1** in  $\text{CDCl}_3$ . The upper spectrum was recorded with the sequence shown in Figure 1b using 70 ms (total duration) sinc shaped pulses (truncated after 3 zero crossings on either side of resonance). The technique is seen to work particularly well. The lower spectrum was recorded under the same conditions, but with a conventional acquisition scheme and can be seen to suffer (as expected for a  $90^\circ$  sinc pulse) from a large phase dispersion in both dimensions. More importantly the upper spectrum recorded with PARADISE is seen to have a significantly greater signal-to-noise ratio. The spectra were recorded with  $1024 \times 128$  (total) points in  $t_2$  and  $t_1$  respectively for a spectral width of  $1000 \times 200$  Hz. For the upper spectrum 35 points were acquired during the pulse in  $t_2$ , and the pulses on either side of  $t_1$  were applied according to the scheme of Figure 1b using 15 steps. Both data sets were zero-filled to  $4k \times 512$  points before apodisation with identical weighting functions and Fourier transformation.  $35 \times 35$  Hz sections are shown in the figure.

spectrum to simulations, as described elsewhere,<sup>3</sup> and the coupling constants we obtain for the NH-H $\alpha$  cross peak in Gramicidin are 9.1 Hz for  $^3J_{\text{NH-H}\alpha}$  and 5.9 Hz for  $^3J_{\text{H}\alpha\text{-H}\beta}$ .

Note that the spectra of Figures 6 and 7 were acquired with presaturation of the water resonance which is essential to avoid contamination by off-resonance artifacts intrinsic to this method. These are usually small in one-dimensional spectra and are strongly attenuated in two-dimensional spectra since they do not give rise to correlations. However, artifacts arising from the large water resonance can be troublesome, hence the requirement for presaturation.

The 57 amino acid Capsid(1-48)\* fragment represents the largest system that has been successfully treated using soft-COSY. Previous reports were able to obtain spectra from some duplex DNA 8-mers only with very long acquisition times (roughly 4 h were required for each cross peak spectrum).<sup>3</sup> Indeed, we were not able to obtain any selective two-dimensional spectrum of the Capsid(1-48)\* using conventional techniques. The spectra of Figure 7, obtained using the sequence of Figure 1 in conjunction with narrowband cosine-bell shaped pulses, therefore represent a significant step upwards in molecular weight. The NH-H $\alpha$  cross peaks shown in Figure 7 were recorded in an experimental time of less than 1 h each on a 3 mM solution. Once again the spectra are of a high quality and are suitable for analysis. The spectra shown are from three different valine residues in the protein and allow the measurement of the active NH-H $\alpha$  and the passive H $\alpha$ -H $\beta$  couplings. For each cross peak we have recorded two different spectra, either interconverting the values of  $\omega_1$  and  $\omega_2$  (yielding spectra from the two symmetrically disposed cross peaks) or using slightly different values for the transmitter offset frequencies.

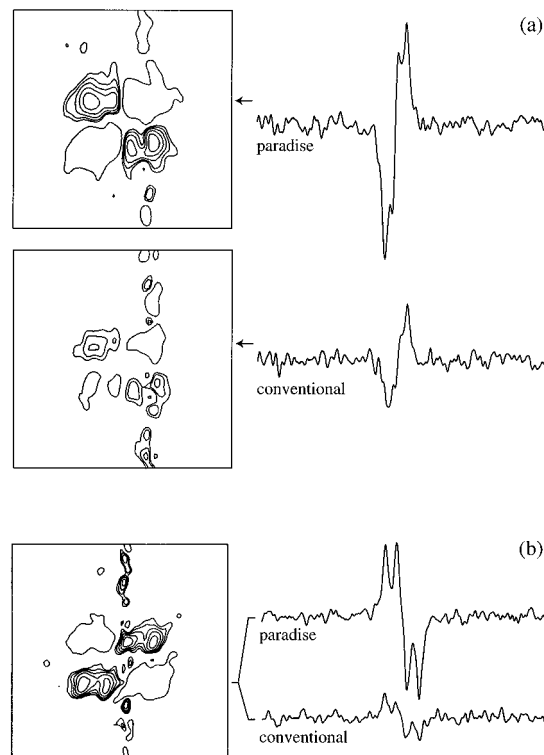


**Figure 6.** Selective COSY spectra for a sample of 2 mM Gramicidin-D from *Bacillus brevis* in 90%  $\text{D}_2\text{O}$ , 10%  $\text{H}_2\text{O}$ . The sample was acquired from Sigma chemical company and used without further purification. (a) Spectra of the valine 8 NH-H $\alpha$  correlation recorded with the sequence shown in Figure 1b using 70 ms (total duration) sinc shaped pulses (truncated after 3 zero crossings on either side of resonance), compared to that obtained using 70 ms UBURP pulses. The PARADISE technique is seen to yield a substantial gain (ca. factor 2) in the signal-to-noise ratio. This gain is all the more remarkable in the spectra (b) of the valine 8 H $\alpha$ -H $\beta$  correlation. In this case the contour plot is only shown for the PARADISE spectrum since at this contour level no discernible signals are observed using the conventional method. Presaturation was applied to eliminate artifacts due to the water resonance. Sixteen scans were used per increment with a two-step phase cycle of the receiver and the first pulse to eliminate axial peaks and a gradient homospoil pulse between the second and third pulses to eliminate transverse coherences. Cross peak frequencies were determined from a low resolution COSY spectrum. The spectra were recorded with  $4k \times 64$  (total) points in  $t_2$  and  $t_1$ , respectively for a spectral width of  $2000 \times 200$  Hz. (Total experimental time for each spectrum = 30 min). For the PARADISE spectra 70 points were acquired during the pulse in  $t_2$ , and the pulses on either side of  $t_1$  were applied according to the scheme of Figure 1b using 15 steps. Both data sets were zero-filled to  $4k \times 512$  points before apodisation with identical weighting functions and Fourier transformation.  $50 \times 50$  Hz sections are shown in the figure.

Thus, we obtain two separate measurements for each of the couplings when the spectra are analyzed by iterative fitting methods, which allows us to estimate the precision of the determination of the coupling constants. As can be appreciated from the results of the fits shown in Figure 7, it appears that 0.3 Hz is a conservative estimate of the precision of the measurement.

The accuracy of the measurements is slightly more difficult to assess. In the case of a DNA sample it was previously reported<sup>3</sup> that the accuracy of measured couplings using soft-COSY determined by independent measurements was between  $\pm 0.22$  and  $\pm 0.45$  Hz. We find that for the polyene (**1**) the measured values are identical to those obtained using nonselective 1D methods. For the peptide sample the values are in agreement with those back calculated from the Karplus rela-

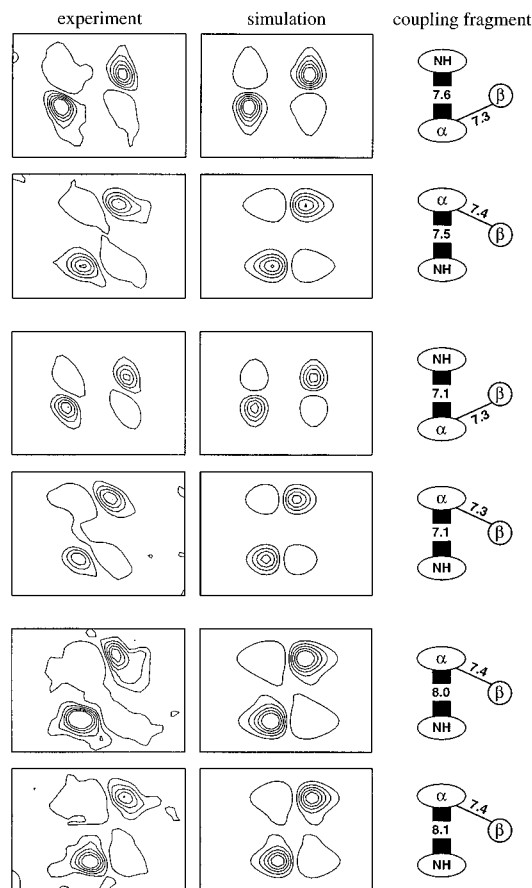


**Figure 7.** Selective COSY spectra for a sample of 3 mM Capsid(1-48)\* in 10% D<sub>2</sub>O, 90% H<sub>2</sub>O. The figure shows the spectra of three of the NH-H $\alpha$  correlations observed for valine residues in the protein. For each correlation, we show two different spectra with, in the case of the upper two groups of spectra, the transmitter frequencies interchanged from one experiment to another so that the two spectra correspond to the two symmetrically disposed cross peaks. In the case of the lower group of two spectra, the transmitter frequencies were changed in both dimensions by a few hertz from one experiment to another. The spectra were recorded using 10 ms cosine-bell shaped pulses, and 21 points were acquired during the pulse in  $t_2$ . The pulses on either side of  $t_1$  were applied according to the scheme of Figure 1b using eight steps. Presaturation was applied to eliminate artifacts due to the water resonance. Sixteen scans were used per increment with a two-step phase cycle of the receiver and the first pulse to eliminate axial peaks and a gradient homospoil pulse between the second and third pulses to eliminate transverse coherences. Cross peak frequencies were determined from a low resolution COSY spectrum. The spectra were recorded with  $4k \times 128$  (total) points in  $t_2$  and  $t_1$ , respectively, for a spectral width of  $4000 \times 700$  Hz. (Total experimental time for each spectrum = 1 h.) Both data sets were zero-filled to  $4k \times 1k$  points before apodisation with identical weighting functions and Fourier transformation.  $45 \times 30$  Hz sections are shown in the figure. On the right hand side of each spectrum is shown the fragment of the coupling network that is determined by iterative fitting of the cross peak to simulations. In the diagram the ovals represent the active spins, directly observed in  $t_1$  and  $t_2$ , and the circles represent passive couplings manifested in the structure of the cross peak.<sup>33,37,38</sup> The precision of the measurement can be appreciated from the differences observed between the two independent measurements of each correlation and appears to be  $< \pm 0.3$  Hz.

tion,<sup>28</sup> and, similarly, for the protein the measured couplings are all physically consistent with the conformation of the backbone in this weakly structured region of the protein. A detailed three-dimensional structure determination for this protein, taking into account constraints obtained from soft-COSY measurements, is in progress.

Currently, the technique most widely used for measuring NH-H $\alpha$  coupling constants in unlabeled proteins is ordinary nonselective DQF-COSY, which is unreliable for large molecules.<sup>30–33</sup> Typically the accuracy of a DQF-COSY measurement is limited by digital resolution which is often about 4 Hz/point in  $t_1$  after zero filling. The exact accuracy of DQF-COSY determinations is difficult to assess, but Majumdar and Hosur<sup>34</sup> have suggested that systematic errors can be as large as 60%. Note that resolution in DQF-COSY can be improved by acquiring many  $t_1$  increments, and nonselective methods could be useful if all the cross peaks in a dense spectrum must be measured accurately. Selective methods are likely to be most useful to provide a few key couplings accurately which relate to areas which pose problems or which require improved accuracy in the structure determination.

The introduction of these new improved sensitivity selective experiments should lead to an appreciable improvement in the accuracy of the measurement of these coupling constants since they have superior digital resolution and yield an E.COSY type cross-peak pattern.<sup>2,3,31,35</sup> We note that all the spectra we present have an E.COSY (or z-COSY) type cross peak pattern in which the active coupling presents an “anti-phase” square pattern, and passive couplings are identified by in-phase displacements of this basic pattern. This represents a significant advantage over the DQF-COSY pattern since the cross peak multiplets may contain less peaks and the structure is particularly well adapted to iterative analysis for the determination of the coupling constants. The routine we use makes use of the symmetry properties of the multiplet.

## Conclusions

We have demonstrated a new method which opens up the possibility of accurately determining structural parameters in significantly larger proteins and DNA fragments than was previously possible using selective NMR correlation techniques. For the example we have studied here, <sup>3</sup>J scalar coupling constants have been measured for a protein with an accuracy of around  $\pm 0.3$  Hz. This method and its derivatives should lead to a corresponding improvement in the precision of molecular structures determined by NMR, as a direct consequence of the very significant sensitivity improvements obtained using the new acquisition techniques introduced here. The sensitivity improvement observed for the 15 amino acid peptide gramicidin leads to a 25-fold reduction in experimental time. In the case of the Capsid(1-48)\* protein sample it was impractical to record spectra without the new technique.

**Acknowledgment.** We are grateful to Dr. Thierry Brodin for the loan of the polyene used in Figure 5 and to Dr. Francois Penin for the Capsid(1-48)\* sample. P.B. is a student following the Magistère des Sciences de la Matière at the Ecole Normale Supérieure de Lyon.

JA961162R

(32) Schmitz, U.; Zon, G.; James, T. L. *Biochemistry* **1990**, *29*, 2357.

(33) Macaya, R. F.; Schultze, P.; Feigon, J. *J. Am. Chem. Soc.* **1992**, *114*, 781.

(34) Majumdar, A.; Hosur, R. V. *Prog. NMR Spectrosc.* **1992**, *24*, 109.

(35) Emsley, L.; Bodenhausen, G. The Role of Selective Two-Dimensional NMR Correlation Methods in Supplementing Computer-Supported Multiplet Analysis by MARCO POLO. In *Computational Aspects of the Study of Biological Macromolecules by Nuclear Magnetic Resonance Spectroscopy*; Hoch, J. C., Ed.; Plenum Press: New York, 1991.

(36) Ernst, R. R.; Bodenhausen, G.; Wokaun, A. *Principles of Nuclear Magnetic Resonance in One and Two Dimensions*; Clarendon Press: Oxford, 1987.

(37) Pfändler, P.; Bodenhausen, G. *J. Magn. Reson.* **1988**, *79*, 99.

(38) Pfändler, P.; Bodenhausen, G. *J. Magn. Reson.* **1990**, *87*, 26.